Ab initio x-ray absorption near-edge structure study of Ti K-edge in rutile

2007 J. Phys.: Condens. Matter 19 266206

(http://iopscience.iop.org/0953-8984/19/26/266206)

IOP PUBLISHING JOURNAL OF PHYSICS: CONDENSED MATTER

J. Phys.: Condens. Matter **19** (2007) 266206 (9pp) doi:10.1088/0953-8984/19/26/266206

Ab initio x-ray absorption near-edge structure study of Ti K-edge in rutile

J Chaboy[1], **N Nakajima**[2] **and Y Tezuka**[3]

[1] Instituto de Ciencia de Materiales de Aragón, CSIC-Universidad de Zaragoza, 50009 Zaragoza, Spain
[2] Graduate School of Science, Hiroshima University, 1-3-1 Kagamiyama, Higashi-Hiroshima 739-8526, Japan
[3] Faculty of Science and Technology, Hirosaki University, 3 Bunkyo, Hirosaki 036-8561, Japan

Received 8 April 2007, in final form 21 May 2007
Published 7 June 2007
Online at stacks.iop.org/JPhysCM/19/266206

Abstract

This work reports a theoretical x-ray absorption near-edge structure (XANES) spectroscopy study at the Ti K-edge in TiO_2 rutile. We present detailed *ab initio* computations of the Ti K-edge XANES spectrum performed within the multiple-scattering framework. An extensive discussion is presented concerning the size of the cluster needed to reproduce the experimental spectrum, especially regarding the split main absorption line. In addition, the role of the exchange and correlation potential (ECP) in reproducing all the experimental XANES features is discussed. The best agreement between experimental data and computations is obtained by using real ECP potentials, i.e. the energy-dependent Dirac–Hara exchange potential, or by using only the real part of the energy-dependent Hedin–Lundqvist complex potential, together with an additional imaginary constant to account for the core-hole lifetime and the experimental resolution. The addition of the imaginary part of the HL potential worsens the agreement between the experimental and calculated spectra, indicating the failure of the complex part of the Hedin–Lundqvist ECP in accounting for the electron damping in these systems.

(Some figures in this article are in colour only in the electronic version)

1. Introduction

Titania (titanium dioxide) is a well-known system intended for use in a wide variety of applications in the field of catalysis and materials science [1, 2]. More recently, TiO_2 has also become a suitable candidate material for different applications such as carbon monoxide sensing elements [3, 4], nano-composite polymer electrolytes [5] or nano-particle-dispersed polyimide composite waveguide materials [6]. Because this interest concerns both crystalline and amorphous TiO_2, x-ray absorption spectroscopy [7] has been used extensively to study the coordination geometry around Ti and the chemical and electronic properties of titanium oxides.

The understanding of the x-ray-absorption near-edge structure (XANES) is a fundamental step into obtaining information regarding the coordination geometries in the amorphous systems. This need motivated the study of XANES spectra of the crystalline oxides having a well-known structure. In this way, the study of the Ti K-edge XANES spectrum of rutile, the stable form of titania, has attracted great attention from both the experimental and theoretical sides. Indeed, the XANES spectrum of rutile presents several pre-edge features whose intensity has been proposed to be related to the coordination number and geometry of the Ti–O polyhedra. However, the interpretation of the pre-edge region of the Ti K-edge XANES spectrum, which is composed of three well-defined features, has been the subject of much debate [8–14]. In a similar way, the interpretation of the near-edge part of the absorption spectrum is also controversial, and several attempts to reproduce theoretically the TiO_2 XANES structures have been reported [8–12, 15–18].

The *ab initio* computation of the XANES spectra requires sophisticated simulation codes [19–23]. Most of these codes are based on the one-electron multiple-scattering (MS) framework [24] and they use the so-called muffin-tin approximation. However, a convincing interpretation of the pre-edge region of Ti K-edge polarized XANES spectra was obtained by using non-muffin-tin calculations based on the finite difference method [13, 14]. By contrast, the debate is still open regarding the reproduction of the Ti K-edge near-edge structures. The early MS computations of TiO_2-rutile reported by Ruiz-Lopez and Muñoz-Páez [9] were made by using a Dirac–Hara exchange potential. In addition, the spectra were convoluted to account for the effect of inelastic losses using the Hedin–Lundqvist approach. The main drawback of these computations was the poor reproduction of the three peaks (C_1, C_2 and D in figure 1) forming the characteristic main absorption line of the Ti K-edge of rutile. Similar results are found in subsequent works, although the methods used to build the scattering potential (cluster-size, overlapping factors, exchange potentials, etc) and the treatment of the damping of the excited photoelectron were different [8–12, 15–18]. Indeed, the treatment of the inelastic losses of the photoelectron still remains an open problem in x-ray absorption spectroscopy (XAS). Typically, these effects are accounted for by using an exchange–correlation potential (ECP). In the case of rutile TiO_2, the energy-dependent Hedin–Lundqvist (HL) complex potential [25, 26] has been the most commonly used. However, it has been reported that in several cases the energy-dependent Dirac–Hara (DH) exchange potential shows the best agreement with the experimental data [9, 27–29], although this assignment is not free of controversy [18, 30–32]. To date, the variety of reported results indicates that this choice is material specific and, unfortunately, prevents one from *a priori* fixing the ECP for each particular case.

In this work, we present a study of the Ti K-edge XANES spectrum in the rutile phase of TiO_2. We have performed detailed *ab initio* computations of the absorption spectra within the multiple-scattering framework. Because of the controversy among previous results, special attention has been paid to the reproduction of the main absorption line concerning both the spectral shape and the relative energy separation and intensity of its different components. The *ab initio*-MS calculations have been performed by using different choices for both the cluster size around the photoabsorbing atom and for the final-state potential. In this way, we have tested different treatments of the exchange–correlation part in the final-state potential, intending to obtain the best agreement both in energy and intensity, between the experimental and theoretical Ti K-edge XANES spectra of TiO_2 rutile.

2. Experimental and computational methods

XANES experiments were performed at the beamline BL-7C of the Photon Factory, KEK Facility. The Ti K-edge XANES spectra of TiO_2 rutile were recorded on powdered samples in

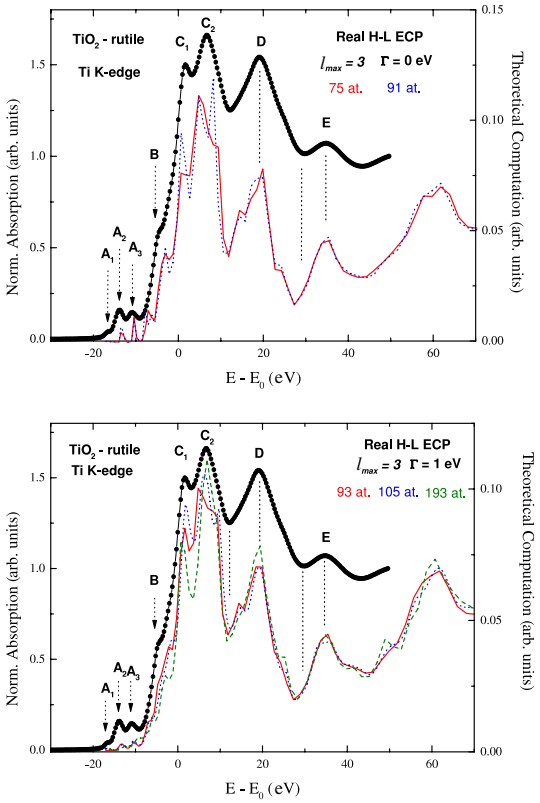

Figure 1. Top panel: Comparison of the experimental Ti K-edge XANES spectrum of TiO_2-rutile (O) and the results of the calculations performed by using the real part of the HL potential for two clusters including 75 (red, solid line) and 91 atoms (blue, dotted line), respectively. Bottom panel: the same comparison is shown for clusters containing 93 (red, solid line), 105 (blue, dotted line) and 193 atoms (green, dashed line). In this case the theoretical spectra have been convoluted with a Lorentzian shape function to account for the core-hole lifetime ($\Gamma = 1.0$ eV).

transmission mode by using a Si(111) double-crystal monochromator. The absorption spectra were analysed according to standard procedures. The origin of the energy scale, E_0, was defined as the inflection point of the absorption edge. The spectra were normalized to the averaged absorption coefficient at high energy, μ_0, in order to eliminate the dependence of the absorption on the sample thickness.

The computation of the XANES spectra was carried out using the multiple-scattering code CONTINUUM [20, 22] based on the one-electron full-multiple-scattering theory [33, 24]. A complete discussion of the procedure can be found in [26] and [34]. Computations were made in parallel mode by using the MPI library [35].

The potential for the different atomic clusters was approximated by a set of spherically averaged muffin-tin (MT) potentials built by following the standard Mattheis' prescription [36]. The muffin-tin radii were determined following Norman's criterion and by imposing an overlapping factor ranging from 1% to 10% [37]. The Coulomb part of each atomic potential was generated using charge densities from the atomic code of non-local self-consistent Dirac–Fock code [38, 39]. The atomic orbitals were chosen to be neutral for the ground-state potential. Two different approximations were tested for the excited state potential: (i) the same potential as for the ground state was used; and (ii) the relaxed $Z + 1$ approximation [40]. During the

present calculations we have found that the screened and relaxed $Z + 1$ option leads to the best performance in simulating the experimental absorption spectra. The exchange and correlation part of the final-state potential has been accounted for by using both the energy-dependent Hedin–Lundqvist (HL) and Dirac–Hara (DH) potentials [26]. The calculated spectra have been further convoluted with a Lorentzian shape function to account for the core-hole lifetime ($\Gamma = 0.94$ eV) [41] and the experimental resolution.

3. Results and discussion

Systematic *ab initio* calculation of the Ti K-edge XANES spectrum was performed for TiO_2 rutile. Titanium dioxide crystallizes in the tetragonal rutile structure (space group $P4_2/mnm$) with a lattice parameter $a = 4.593$ Å [42]. The Ti atoms are located at the centre of a distorted octahedron forming an TiO_6 cluster. The coordination oxygen octahedron around the titanium atom is slightly distorted, the two apical Ti–O distances (1.98 Å) being slightly greater than the four equatorial distances (1.95 Å).

The experimental XANES spectrum at the Ti K-edge of TiO_2 is shown in figure 1. The spectrum is characterized by the existence of three peaks at the pre-edge region whose origin has been discussed at length in the past. In addition, the spectrum shows a shoulder-like feature (B) at the raising edge and a split (C_1, C_2) main absorption line. Moreover, there are a broad asymmetric resonance (D) and a weak peak (E) at ∼20 and ∼35 eV above the edge, respectively.

Different computations of the Ti K-edge XANES spectrum of rutile have been reported in the past [8–12, 15–18]. A common characteristic of these works, with the exception of that of Aifa *et al* [17], is the use of small-medium size clusters and their failure in reproducing the C_1 structure of the main absorption line. According to Ruiz-Lopez and Muñoz-Páez [9], at least 51 atoms should be included in the computations in order to get all the spectral features. This model includes all atoms lying in a radius of 5.5 Å around photoabsorbing Ti, so that one can consider that scattering paths of total length greater than ∼11 Å contribute little to the absorption. A similar conclusion has recently been reached by Farges *et al* by using a cluster of 59 atoms [10]. However, these computations do not reproduce the peak E (∼35 eV) and the energy separation among the different spectral features, as well as their relative intensities, are not properly reproduced.

We have initially optimized the size of the cluster needed to reproduce all the structures present in the experimental XANES spectrum. We have performed calculations by increasing progressively the number of atoms up to and including 193 atoms covering a range of ∼7.52 Å around the absorbing Ti. (For this computation we have used the real part of the Hedin–Lundqvist potential. The using of a real potential is motivated because its imaginary part may introduce an excessive and unrealistic damping of the signal, resulting in the hindering of weak absorption features.) In this way, figure 1 shows how all the spectral features, including C_1, are accounted for by using a 91 atoms cluster, i.e. including the Ti and O atoms located within the first 5.85 Å around the photoabsorbing Ti. By contrast, the computation performed for a smaller cluster containing 75 (5.5 Å) does not account for the C_1 structure. The addition of further coordination shells does not introduce new spectral features, but mainly affects both the spectral shape and the intensity ratio of the two C_1 and C_2 contributions to the split main absorption line. As shown in figure 1, the computation performed for a cluster containing 105 atoms (6.5 Å) accurately reproduces the shape of the main C_2 peak, in contrast to that performed by using only 93 atoms (5.93 Å). Finally, no significant modification is observed by increasing the cluster size to 193 atoms (7.52 Å) and only the relative intensity of the different spectral features is concerned.

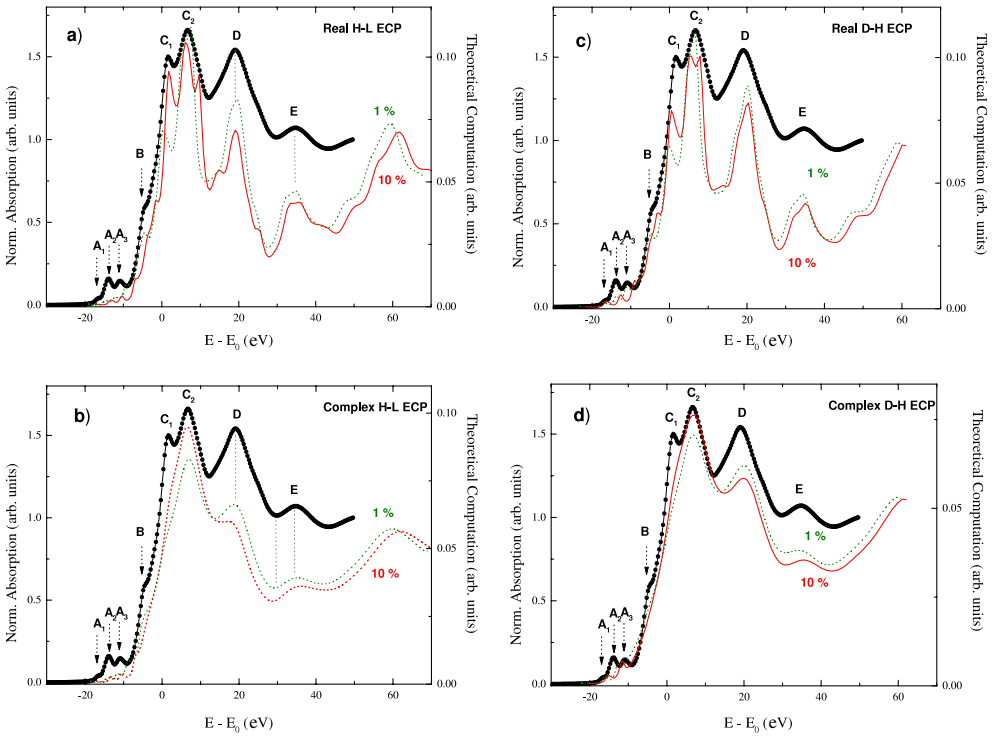

Figure 2. Comparison of the experimental Ti K-edge XANES spectrum of TiO_2-rutile (○) and the results of the calculations performed by using different ECPs for a cluster (105 atoms) covering up to 6.5 Å around the absorbing Ti: (a) real HL, (b) complex HL, (c) real DH and (d) *complex* DH. In all the cases, computations have been performed by imposing an overlapping factor of 1% (green, dotted line) and 10% (red, solid line), and a ($\Gamma = 1.0$ eV) broadening (see text for details).

Based on the above results, we have fixed the cluster size to 6.5 Å (105 atoms) around the photoabsorber to test the performance of different exchange and correlation potentials (ECP) to account for the experimental spectrum. We have computed the Ti K-edge XANES of rutile by using both energy-dependent Hedin–Lundqvist (HL) and Dirac–Hara ECP potentials [26]. The HL is a complex potential in which its imaginary part accounts for the inelastic losses of the photoelectron. However, it has been reported that in several cases the damping of the signal simulated in this way is excessive [34]. For the same reason, we have also performed computations by using only the real part of the HL ECP (hereafter, real HL). Conversely, because DH is a real ECP, we have built a '*complex*' DH one by adding to the standard energy-dependent Dirac–Hara exchange potential, the imaginary part of the HL ECP. Prior to performing these calculations, we have determined the maximum angular momentum quantum number for the 105 atoms cluster, l_{max}, needed to account for the experimental spectrum in the first 100 eV of the absorption spectrum. We have verified that the choice of $l_{max} = 3$ and 4 does not affect the result of the computations in the first 50 eV of the spectrum above the edge. Accordingly, all the calculations reported henceforth have been obtained by fixing $l_{max} = 3$ and convoluted with a Lorentzian function ($\Gamma = 1$ eV).

Figure 2 shows the comparison of the experimental spectrum and the calculations performed for the four different ECPs. Both real HL and DH potentials reproduce all the spectral features shown by the experimental spectrum. The calculations reproduce the shoulder-like feature (B) at the threshold, both C_1 and C_2 peaks of the main absorption structure, and

the broad resonances (D and E) at higher energies. The performance of both potentials is similar, the main difference between these calculations being the reproduction of both the intensity ratios and the relative energy separation among the spectral features. The agreement between the experimental and theoretical spectra clearly worsens by using a complex potential. As shown in figure 2, the introduction of the imaginary part of the HL potential induces an over-damping of the signal. As a consequence, the C_1 structure is completely suppressed and feature B blurs. This result is independent of the choice of the real part (HL or DH) of the ECP potential. We have verified that this effect is not due to the choice of the overlapping factor among the muffin-tin spheres. To this respect we have performed the computations by imposing different overlapping factors. The use of both 1% and 10% factors leads to the same results concerning the excessive damping of XANES by using complex potentials. However, the choice of the factor affects both the intensity and the spectral shape in the first 25 eVs of the computed spectra. Computations performed by using a 10% factor show better agreement with the experimental spectrum than those corresponding to a 1% overlapping factor. In the latter case, the reproduction of the C_1/C_2 intensity ratio clearly worsens and, in addition, the asymmetric shape of both C_2 and D peaks is not accounted for by the computation.

As a final verification of the above results we have extended our calculations to a bigger cluster. In this way, we have performed the Ti K-edge computation by using: (i) 193 atoms, covering a range of ∼7.52 Å around the absorbing Ti, to build the cluster; (ii) $l_{\max} = 3$; and (iii) the 10% overlapping factor. Moreover, the effect of both the core-hole lifetime (0.94 eV) and the experimental resolution (1 eV) has been accounted for by convoluting the calculated spectra with a Lorentzian broadening function ($\Gamma = 1.4$ eV). These calculations have been performed by using the four different exchange and correlation potentials, as described above. The results, shown in figure 3, indicate that the best agreement between the calculations and the experimental spectrum is obtained by using real ECP potentials, i.e. the energy-dependent Dirac–Hara exchange potential or by using only the real part of the energy-dependent Hedin–Lundqvist complex potential. In all the cases, contrary to previous claims, the addition of the imaginary part of the HL potential worsens the agreement. The performance of both real HL and DH into reproducing the experimental spectrum is similar concerning both the intensity ratio and the relative energy separation among the different spectral features. Nevertheless, based on these criteria, the computation performed by using only the real part of the HL ECP yields the best agreement with the experimental data. As shown in figure 4, the computation performed by using the real part of the HL ECP perfectly reproduces the relative energy separation among C_1, C_2, D and E spectral features as well as with the relative absorption minima. In the case of the simulations carried out with the Dirac–Hara potential, the spectra are slightly expanded with respect to the experimental one. In addition, the asymmetric shape of the D resonance (arrow mark in figure 4) is better reproduced by using the real HL ECP than the DH one. Finally, we have performed the same class of computation but using for the final state the same potential as for the ground state, i.e. without any core-hole. As shown in figure 4 the calculation worsens in the absence of the core-hole. In particular, the shape of the C_2 is not well reproduced and the position of both peaks C_2 and D are shifted to higher energies than that observed experimentally.

4. Summary and conclusions

We have presented the detailed *ab initio* computation of the Ti K-edge XANES spectrum in the case of TiO_2-rutile performed within the multiple-scattering framework.

The comparison between the experimental data and our *ab initio* computations indicates the need of using large clusters to reproduce the experimental spectrum, especially regarding feature C_1 of the split main absorption line. This result is in agreement with that of Aifa *et al*

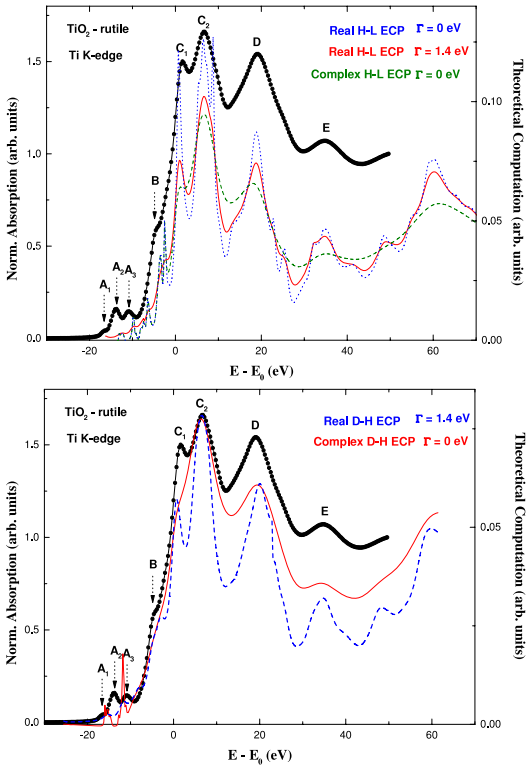

Figure 3. Top panel: comparison of the experimental Ti K-edge XANES spectrum of TiO_2-rutile (○) and the computations performed for a 7.52 Å (193 atoms) cluster by using both real HL (blue, dotted line) and complex HL (green, dashed line). For the sake of completeness, the real HL computation after convolution (red, solid line) is also shown (see text for details). Bottom panel: similar comparison is shown for computations obtained by using real (blue, dash) and *complex* (red, solid line) Dirac–Hara exchange and correlation potential.

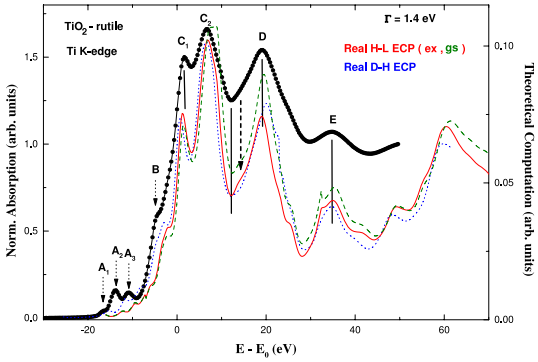

Figure 4. Top panel: comparison of the Ti K-edge XANES spectra computed for a 7.52 Å TiO_2-rutile cluster by using both DH (blue, dotted line) and the real part of the HL potential (red, solid line). For the sake of completeness the computation obtained by using the same potential as for the ground state is also shown (green, dashed line).

[17] and shows the inadequacy of small- [18] and medium-size clusters [9, 10] to properly account for the spectral shape of rutile.

In addition, we have tested different treatments of the exchange and correlation contribution to construct the final state potential. The best agreement with the experimental data has been obtained by using real ECP potentials, i.e. the energy-dependent Dirac–Hara exchange potential or by using only the real part of the energy dependent Hedin–Lundqvist complex potential, together with an additional imaginary constant ($\Gamma = 1.4$ eV) to account for the core-hole lifetime and the experimental resolution. The intensity ratio between the C_1 and C_2 peaks is well reproduced by using both real HL and DH ECP potentials. However, the relative energy separation among the different spectral features results is excessively expanded by using the Dirac–Hara ECP. Contrary to previous claims, the addition of the imaginary part of the HL potential worsens the agreement between the experimental and calculated spectra, indicating the failure of the complex part of the Hedin–Lundqvist ECP in accounting for the electron damping in these systems.

Acknowledgments

This work was partially supported by the Spanish CICYT MAT2005-06806-C04-04 grant. JCh acknowledges a fellow from the Japanese Society for the Promotion of Science: Invitation Fellowship Program for Research in Japan.

References

[1] Kung H 1989 *Transition Metal Oxides* vol 45, ed B Delmon and J Yates (Amsterdam: Elsevier)
[2] Foger K 1984 *Catal. Sci. Technol.* **6** 227
[3] Dutta P K, Ginwalla A, Patton B R, Chwieroth B, Liang Z, Gouma P, Mills M and Akbar S 1999 *J. Phys. Chem.* B **103** 4412
[4] Gouma P I, Dutta P K and Mills M J 1999 *Nanostruct. Mater.* **11** 1231
[5] Johansson P and Jacobsson P 2004 *Solid State Ion.* **170** 73
[6] Yoshida M, Lal M, Deepak Kumar N and Prasad P N 1997 *J. Mater. Sci.* **32** 4047
[7] For a review see for example, Prins R and Koningsberger D (ed) 1988 *X-Ray Absorption: Principles, Applications, Techniques of EXAFS, SEXAFS, XANES* (New York: Wiley) and references therein
[8] Brydson R, Sauer H, Engel W, Thomas J M, Zeitler E, Kosugil N and Kurodal H 1989 *J. Phys.: Condens. Matter* **1** 797
[9] Ruiz-Lopez M F and Muñoz-Páez A 1991 *J. Phys.: Condens. Matter* **3** 8981
[10] Farges F, Brown G E Jr and Rehr J J 1997 *Phys. Rev.* B **56** 1809
[11] Poumellec B, Durhamn P J and Guo G Y 1991 *J. Phys.: Condens. Matter* **3** 8195
[12] Wu Z Y, Ouvrard G, Gressier P and Natoli C R 1997 *Phys. Rev.* B **55** 10382
[13] Cabaret D, Joly Y, Renevier H and Natoli C R 1999 *J. Synchrotron Radiat.* **6** 258
[14] Joly Y, Cabaret D, Renevier H and Natoli C R 1999 *Phys. Lett.* **82** 2398
[15] Bohr F, Ruiz-Lopez M F and Muñoz-Páez A 1993 *Catal. Lett.* **20** 59
[16] Wu Z Y, Ouvrard G and Natoli C R 1997 *J. Physique Coll.* IV **7** C2 199
[17] Aifa Y, Poumellec B, Jeanne-Rose V, Cortes R, Vedrinskii R V and Kraizman V L 1997 *J. Physique Coll.* IV **7** C2 217
[18] Jeanne-Rose V and Poumellec B 1999 *J. Phys.: Condens. Matter* **11** 1123
[19] Vvedensky D D, Saldin D K and Pendry J B 1986 *Comput. Phys. Commun.* **40** 421
[20] Natoli C R and Benfatto M, unpublished
Benfatto M, Natoli C R, Bianconi A, García J, Marcelli A, Fanfoni M and Davoli I 1986 *Phys. Rev.* B **34** 5774
[21] Ankudinov A L, Ravel B, Rehr J J and Conradson S D 1998 *Phys. Rev.* B **7565**
[22] Benfatto M and Della Longa S 2001 *J. Synchrotron Radiat.* **8** 1087
Della Longa S, Arcovito A, Girasole M, Hazemann J L and Benfatto M 2001 *Phys. Rev. Lett.* **87** 155501
[23] Joly Y 2001 *Phys. Rev.* B **63** 125120
[24] Lee P A and Pendry J B 1975 *Phys. Rev.* B **11** 2795
[25] Hedin L and Lundqvist B 1971 *J. Phys. C: Solid State Phys.* **4** 2064
[26] Natoli C R, Benfatto M, Della Longa S and Hatada K 2003 *J. Synchrotron Radiat.* **10** 26
[27] Gunnella R, Benfatto M, Marcelli A and Natoli C R 1990 *Solid State Commun.* **76** 109

[28] Díaz-Moreno S, Muñoz-Páez A and Chaboy J 2000 *J. Phys. Chem.* A **104** 1278
[29] Briois V, Sainctavit Ph and Flank A-M 1993 *Japan. J. Appl. Phys. Suppl.* **32** 52
[30] Chaboy J, Benfatto M and Davoli I 1995 *Phys. Rev.* B **52** 10014
[31] Cabaret D, Sainctavit Ph, Ildefonse Ph and Flank A-M 1996 *J. Phys.: Condens. Matter* **8** 3691
[32] Cabaret D, Le-Grand M, Ramos A, Flank A-M, Rossano S, Galoisy L, Calas G and Ghaleb D 2001 *J. Non-Cryst. Solids* **289** 1
[33] Natoli C R and Benfatto M 1986 *J. Physique Coll.* **47** C8 11
[34] See for example Chaboy J and Quartieri S 1995 *Phys. Rev.* B **52** 6349 and references therein
[35] See for example http://www-unix.mcs.anl.gov/mpi/
[36] Mattheis L F 1964 *Phys. Rev.* A **133** 1399
Mattheis L F 1964 *Phys. Rev.* A **134** 970
[37] Norman J G 1974 *Mol. Phys.* **81** 1191
[38] Desclaux J P 1975 *Comput. Phys. Commun.* **9** 31
[39] Ankudinov A L, Ravel B, Rehr J J and Conradson S D 1998 *Phys. Rev.* B **58** 7565
[40] Lee P A and Beni G 1977 *Phys. Rev.* B **15** 2862
[41] Krause M O and Oliver J H 1979 *J. Phys. Chem. Ref. Data* **8** 329
[42] Howard C J, Sabine T M and Dickson F 1991 *Acta Crystallogr.* B **47** 462